15A.4 Partial Beam Blockage Correction Using Dual-Polarimetric Measurements

Pengfei Zhang[1], Dusan Zrnic[2], Alexander Ryzhkov[1]

[1]CIMMS, University of Oklahoma, Norman, Oklahoma
[2]NOAA's National Severe Storms Laboratory, Norman, Oklahoma

1. Introduction

Beam blockage caused by terrain and other obstacles such as buildings and trees limits radar coverage and introduces bias in measurements. The national network of S-band operational WSR-88D (Weather Surveillance Radar-1988 Doppler) radars, especially in the mountainous western United States is severely affected by beam blockage. The accuracy of the weather radar products such as quantitative precipitation estimates (QPE) (Westrick et al. 1999, Young et al. 1999, Pellarin et al. 2002) and vertically integrated liquid (VIL) estimates is compromised. The dual polarization being implemented on the network has the potential to mitigate this problem. Dual-polarimetric radar has been demonstrated to produce better QPEs by using specific differential phase in the beam blockage area and the presence of anomalous propagation than current single polarimetric WSR-88D radar (Zrnic and Ryzhkov 1996, Ryzhkov and Zrnic 1996, Ryzhkov and Zrnic 1998, Vivekanandan et al. 1999).

On weather radars, digital elevation map (DEM) is often used to correct reduced reflectivity caused by radar beam blockage. Two ways of making the correction have been proposed. One consists of using DEM and partitioning the radar volume scan region into blocked and unblocked parts. Then a vertical profile of reflectivity (VPR) in the unblocked region is constructed and used to estimate the reflectivity in blocked region (Andrieu et al. 1997; Creutin et al. 1997; Kucera et al. 2004). The other way is to estimate beam blockage percentage by using the DEM and radar beam geometry (Bech et al. 2003); these authors have studied the impact of variability of surrounding vertical refractivity gradient on the sensitivity of their beam blockage correction and found the correction to be fairly robust.

With dual-polarimetric radar measurements, many QPE methods based on the immunity of specific differential phase to PBB (partial beam blockage) have been developed (Carey et al. 2000; Giangrande and Ryzhkov 2005; Lang et al. 2009). Fundamental to these methods is a self-consistency relation between reflectivity factor Z_h in horizontal channel and specific differential phase K_{dp} expected to hold in rainfall (Goddard et al. 1994; Scharchilli et al. 1996; Ryzhkov et al. 2005).

Ideas to use differential phase Φ_{DP} or specific differential phase K_{DP} directly for computing rainfall have been put forward but not sufficiently tested. An obvious impediment with these is the uncertainty caused by fluctuations in the Φ_{DP} or K_{DP} estimates. We propose a new method that uses the integration of the self-consistency relationship over each radar beam to estimate beam blockage fraction (BBF thereafter) dynamically and then correct measured reflectivity factor in the blocked area. Instead of applying self-consistency relationship at each radar gate, the integration mitigates the uncertainty of the Φ_{DP} or K_{DP} measurements and improves the accuracy and steadiness of the BBF estimations.

2. Methodology

The method is based on the general idea of consistency between Z, specific differential phase K_{DP}, and differential reflectivity Z_{DR} in rain (Ryzhkov et al. 2005). The concept of self-consistency can be utilized for correcting Z bias caused by radar miscalibration, attenuation, and partial beam blockage. It has been successfully

**Corresponding author address*: Pengfei Zhang CIMMS, University of Oklahoma, Norman, OK 73072; e-mail: Pengfei.Zhang@noaa.gov

implemented and tested in more recent studies by Lang et al. (2009) and Marks et al. (2010).

According to the consistency concept, Z, Z_{DR}, and K_{DP} are interdependent in pure rain so that

$$K_{DP} = aZ^{b}Z_{dr}^{c}, \qquad (1)$$

where Z and Z_{dr} are expressed in linear units (Z is in mm^{6}m^{-3} and K_{DP} is in deg km^{-1}). The coefficients in Eq.(1) are relatively insensitive to variability of drop size distributions. Left-hand and right-hand parts of Eq. (1) are equal if both Z and Z_{dr} are perfectly calibrated and are not biased by attenuation / differential attenuation. Checking the consistency locally (i.e., on the gate-to-gate or pixel-by-pixel basis) is limited to the areas of moderate-to-heavy rain (at S and C bands) where the estimates of K_{DP} are less noisy. In order to avoid such a limitation and make consistency check reliable in any rain regardless of its intensity, Ryzhkov et al. (2005) suggested to compare the integrals of left and right sides of Eq. (1) over sufficiently large temporal / spatial domain

$$\int K_{DP} dr = \int aZ^{b}Z_{dr}^{c} dr . \qquad (2)$$

In practice, it is more advantageous to integrate along radials of the radar data so that the integral in the left side of Eq. (2) is proportional to total differential phase Φ_{DP} which is a very robust radar measurement:

$$2\int K_{DP} dr = \Phi_{DP} = 2\int aZ^{b}Z_{dr}^{c} dr . \qquad (3)$$

Using Φ_{DP} is convenient to sort out unblocked and blocked azimuthal directions and to select the radials which are suitable for consistency check, i.e., those where attenuation is not significant. The problem in utilization of Eq. (3) for absolute calibration of Z in the areas affected by PBB is that differential reflectivity Z_{DR} is commonly affected by PBB as well (Giangrande and Ryzhkov 2005). The related Z_{DR} bias for each partially blocked azimuthal direction has to be eliminated first.

Therefore, we resort to a relatively simple and robust algorithm for PBB correction which capitalizes on the ideas from the previous studies and which can be utilized operationally with minimal effort. In a nutshell, the method is based on the use of the power-law K_{DP} – Z relation (Ryzhkov et al. 1997)

$$K_{DP} = aZ^{b} \qquad (4)$$

with variable intercept a which is determined on the scan-to-scan basis using the data in the unblocked azimuthal directions. Assuming the variations of intercept parameter of rain drop size distribution and atmospheric temperature within a radar scan is insignificant, the parameter a can be set to a constant. The parameter b is also assumed to be a constant with the value of 0.72 for S band radar. If Z is well calibrated and is not biased by attenuation, then the parameter a can be estimated by integrating K_{DP} (i.e., Φ_{DP}) and Z^{b} along radials and instead of estimation based on local values of Z and K_{DP} in the unblocked area,

$$a = \frac{\Phi_{DP}(r_m) - \Phi_{DP}(r_o)}{2\int_{r_0}^{r_m} Z^{b}(s)ds}. \qquad (5)$$

In blocked area, the measured reflectivity factor Z becomes smaller and can be written as the product of (1-BBF) and unblocked (or restored) reflectivity factor Z. BBF is a fraction of the beam cross section (defined with the 3 dB contour) being blocked. Here the parameter a is redefine as a_B and for each blocked radial it is estimated as,

$$a_B = \frac{\Phi_{DP}(r_m) - \Phi(r_{0B})}{2\int_{r_{0B}}^{r_m} [(1-BBF)Z(s)]^{b} ds}, \qquad (6)$$

where r_{0B} represents the starting range of beam blockage for the blocked radials. Note that multiple blockages with increasing blockage faction with range along a radial are not considered here. It is evident that parameter a_B is larger than a because Φ_{DP} measurements are not affected by blockage while the integral in the denominator decreases due to beam blockage.

The parameter *a* may vary from storm-to-storm and, strictly speaking, between successive scans and individual radials due to the impact of the variability in drop size distributions. So in our method the mean or median value of the parameter *a* is determined scan by scan based on (5) from the azimuths where blockage is absent. Then the BBF can be obtained for each blocked radial via

$$BBF = 1 - \left(\frac{a}{a_B}\right)^{\frac{1}{b}} . \qquad (7)$$

The bias ΔZ can be estimated as

$$\Delta Z(dB) = \frac{10}{b}\log\left(\frac{a_B}{a}\right) \qquad (8)$$

along the radial in the blocked azimuth.

3. **Application**

a. Case test

During the SoWMEX/TiMREX (Southwest Monsoon Experiment/Terrian-influenced Monsoon Rainfall Experiment) in June 2008, NCAR SPOL (S-band POLarimetric Doppler radar system) radar made dual-polarimetic measurements of several precipitation events in the western plain and mountainous region of southern Taiwan. SPOL radar was deployed on the west side of the Central Mountain Range. The radial resolution of the data was 150 m and azimuthal resolution was 0.91^o. The east side of radar scans at the several lowest elevation angles was partially or totally blocked by the mountains. A DEM for SPOL radar in a polar coordinate system has been generated from the GIS (Geographic Information System) with spatial resolution of about 270 m. Then the beam blockage maps for SPOL at this location with elevation and azimuth resolution of 0.1^o and range resolution of 1 km were produced. Fig.1 illustrates the BBF of SPOL radar at the elevation angles of 0.5^o and 1.1^o. Attenuation caused by rain and gas was insignificant for S-band SPOL radar for the selected cases and was not considered in this study.

To assess the performance of our method, a large precipitation area observed by SPOL at 12:00 UTC on June 14, 2008 is selected. It can be seen in Fig.1 that at elevation angle of 0.5^o radar beam is partially or totally blocked in about two thirds of the radar coverage area. Following the methodology introduced in the previous section, the parameters *a* and a_B were calculated for each radial in the clear and partially blocked areas. The estimated parameters *a* and a_B are shown at each azimuth for the entire radar scan at 0.5^o in Fig.2a. Note that the DEM data are used here to determine which beam is blocked and the starting range (r_{oB} in Eq. (6)) of blockage for the beams. Here the median value of parameter *a* estimated in the unblocked area is 4.21×10^{-4} for this radar scan. Comparing the BBF estimated using our method in the partially blocked sector with the estimates from DEM, the azimuthal dependence of estimated BBF is consistent with the one obtained from DEM (Fig.2b) except within the azimuthal interval between 262^o and 315^o .

To closely examine the difference of BBFs derived between our method and DEM, the values of BBF at azimuths between 250^o and 340^o are magnified and shown in Fig.3. It is obvious that most of BBFs estimated using our method (open squares) is higher than the BBFs derived from DEM (solid dots). To understand the discrepancy, we have superposed beams of SPOL radar in three dimensions on Google Earth. The radar beam propagation path is calculated under standard atmospheric condition based on the equations described by Doviak and Zrnic (2006).

By examining the geographic information provided by Google Earth on the paths between 250^o and 340^o, we found that except for the mountains that are accounted in the DEM estimation, there are many high rise buildings in downtown of Kaohsiung City that are not accounted in DEM, but are on the paths of these blocked radar beams and cause extra blockage between the azimuths of 290^o and 320^o. These buildings are also observed by SPOL radar and can be identified by strong echoes in the unfiltered reflectivity factor field (not shown). This suggests that our BBF estimates are more accurate than the estimates from the DEM.

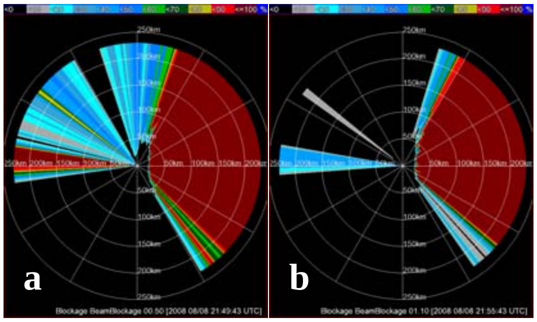

FIG.1. Beam blockage fraction for SPOL radar at elevation angle of (a) 0.5^o and (b) 1.1^o.

Fig.4 illustrates the propagation path of SPOL at the azimuth of 305^o and the elevation angle of 0.5^o on Google Earth display. Along the radar beam illustrated by blue rays, it can be found that except mountains marked by red ellipse there are two high rise buildings highlighted by the red box. The two blue rays represent the radar beamwidth of 0.91^o. The yellow lines divide the path into radar gates with width of 150 m.

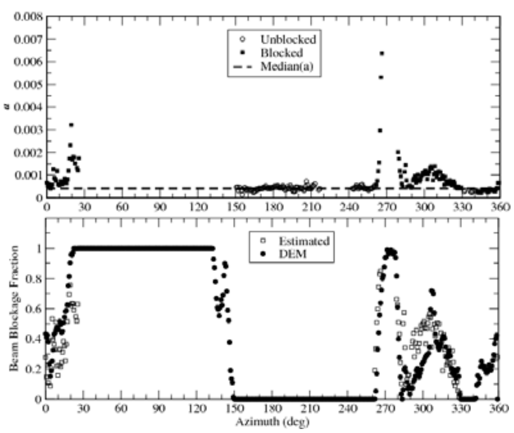

FIG.2. a) Estimated parameter *a* (open circles) in the unblocked azimuths and parameter a_B (solid squares) in the blocked azimuths. The dash line indicates the median value of parameter *a* obtained in the unblocked area. b) Beam blockage fraction obtained from DEM (solid dots) and derived from our method (open squares) in each azimuth. The radar data used to estimate parameter a, a_B and BBF were observed at 12:00 UTC on June 14, 2008 at elevation angle of 0.5^o.

Another cause of BBF discrepancy between our and DEM estimation is that BBF is estimated with respect to the 0.91^o beamwidth weighted with radar power density distribution. It means that the radar transmitted/received power beyond the beamwidth is not accounted for the BBF estimation in DEM method. Our estimation is based on the dual-polarimetric radar measurements with true radar power density distribution within radar beams.

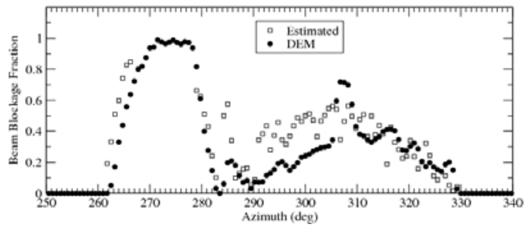

FIG.3. Same as Fig.2b, but azimuth is between 250^o and 340^o.

FIG.4. Radar beam propagation path of SPOL in Taiwan at the azimuth of 304.5^o and the elevation angle of 0.5^o. Two high rise buildings and mountains blocking the radar beam are marked by the red box and ellipse respectively. The two blue rays represent the radar beamwidth of 0.91^o. The yellow lines divide the path into radar gates with width of 150 m.

Using the estimated BBF, the beam blockage correction is applied to the reflectivity factor field. Fig. 5 displays the measured and corrected reflectivity fields at 12:00 UTC from June 14, 2008 at elevation angles of 0.5^o. Clearly, the gap caused by severe blockage in the measured reflectivity at elevation angle of 0.5^o and around azimuth of 270^o is filled by the corrected reflectivity at those beams. The continuity of radar echo patterns is recovered and shows the success of the correction. However the reflectivity along the beam in several azimuths is not recovered because the measured total $\Delta\Phi_{DP}$ is too small to satisfy the given threshold of 5^o. The DEM information showed in Fig. 3 indicates that those beams might be totally blocked. Closely comparing the measured and corrected reflectivity fields in the partial blockage area at the azimuth between 280° and 320°, it has been found that measured reflectivity is enhanced to some degree. The quantitative evaluation is discussed in the following section.

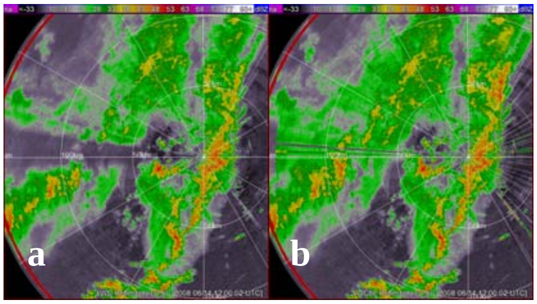

FIG.5. (a) Measured reflectivity fields of SPOL at 12:00 UTC on June 14, 2008; elevation angle is 0.5°, and (b) corrected reflectivity fields at elevation angle of 0.5°. The range rings are 50 km apart.

4. Evaluation of correction

a. Artificial case test

To quantify the performance of our method, an artificial beam blockage test is designed. The received power is artificially reduced by 90% and 99% in the sector from azimuth of 200° to 205° at 0.5° elevation angle starting at 30 km from the radar where the radar beams are not blocked originally. The 90% and 99% reductions in the received power are equivalent to 10 and 20 dB loss in reflectivity factor. Fig.6b displays the 20 dBZ loss in the specified sector. These beams are intentionally selected in the area with relatively strong radar echoes (~30 dBZ). Thus the Φ_{DP} difference and integral term of Eq. (5) or (6) are large enough not only to satisfy the thresholds in the algorithm, but also to reduce the errors in the estimations.

Then our method is applied to correct the reflectivity factor at the artificially blocked radar beams. Comparing Fig.6a with Fig.6c, it can be seen that the reduced reflectivity is totally restored. To quantitatively assess accuracy of the correction, the restored reflectivity for each blocked beam is listed in Table 1. The compensations are not exactly 10 or 20 dBZ at these radar beams, and vary beam by beam within about 1.5 dB as functions of azimuth. The uncertainty in the assumptions such as constant parameter *a* made in the section 2 and errors in the radar measurements may result in the difference between original and corrected reflectivity.

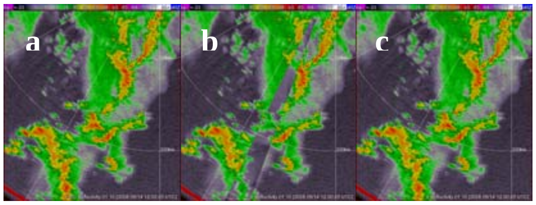

FIG.6. (a) Measured reflectivity, (b) reflectivity as in a) but reduced by 20 dB between azimuths 200° and 205°, and (c) restored reflectivity. The observation time is the same as in Fig. 5.

b. Comparison between upper and lower scans

Besides the artificial case test, we have also employed the comparison of the reflectivity factor observations at the scans between lower (0.5°) and upper (1.1°) elevation angles to qualitatively evaluate the performance of our method. First, the radar horizontal coverage is partitioned into three areas: 1) unblocked area for both scans (area 1 thereafter); 2) unblocked at upper scan and partially blocked at lower scan (area 2 thereafter); 3) the rest of the scan. Second, comparing the reflectivity factors at the same horizontal locations between lower and upper scans in the areas, the statistical relations between them can be found. To avoid the contaminations of ground clutter, melting layer, and non-meteorological scatterers, only the reflectivity factor measurements with the corresponding cross-correlation coefficient larger than 0.9 at the range between 50 and 100 km are selected for the comparison. Fig.7 displays the scatterplot of reflectivity factor at the elevation of 0.5° vs. 1.1° in the area 1 observed by SPOL radar at 12:00 UTC on 14 June 2008. Clearly the points are evenly distributed about the diagonal line implying the reflectivity factors at the lowest two scans (0.5° and 1.1°) are almost identical at the same horizontal location. In other word, there is no significant vertical change in reflectivity factor within 100 km range for this measured rain event at the lowest two elevation angles. The ratio (Z_{upper}/Z_{lower} ratio thereafter) between the total reflectivity at upper and lower scans in the area 1 is 1.04 that is very close to 1. Here the total reflectivity is the sum of measured reflectivity factor in dBZ at each radar gate in the area 1 and 2.

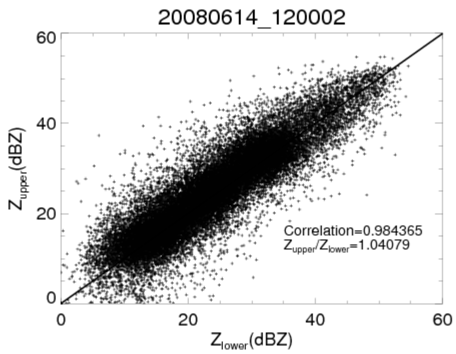

FIG.7. Scatterplot of reflectivity factor at the elevation of 0.5° vs. 1.1° in the unblocked area at 12:00 UTC on 14 June 2008.

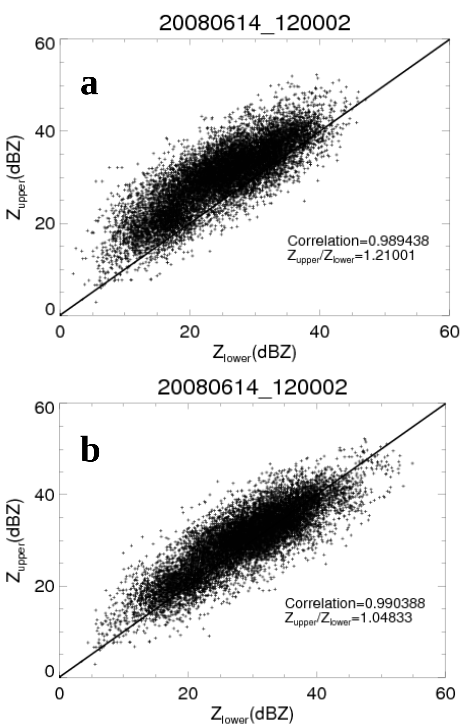

FIG.8. Scatterplots of (a) measured and (b) corrected reflectivity factor at the elevation of 0.5° vs. 1.1° in the area 2 at 12:00 UTC on 14 June 2008.

Then the comparison is conducted in the area 2 and displayed in Fig.8. The measured reflectivity factor comparison in the area 2 is illustrated in Fig.8a. Obviously, reflectivity factors are smaller at the lower scan than the upper scan due to power loss caused by beam blockage. The Z_{upper}/Z_{lower} ratio is 1.21 that is about 16% larger than 1.04 in the area 1. Contrast to it, Fig.8b exhibits the comparison between measured reflectivity factors at upper scan and the reflectivity factors corrected using our method at lower scan in the area 2. The entire cluster of point clearly shifts to the diagonal line because of the beam blockage correction at the lower scan. The Z_{upper}/Z_{lower} ratio is reduced from 1.20 to 1.05 which is close to 1.04 obtained in the area 1. Similar results are also obtained for the other scans observed by SPOL radar in the SoWMEX/TiMREX. The Z_{upper}/Z_{lower} ratio in the area 1 and area 2 before and after beam blockage correction for 45 radar volume scans have been estimated. Comparing with the Z_{upper}/Z_{lower} ratios in area 2 without the correction, most of the Z_{upper}/Z_{lower} ratios after the correction are much closer to the ratio in the unblocked area 1. Although some ratios are away from 1.04, it indicates the uncertainties in our scheme. The average Z_{upper}/Z_{lower} ratio over these 45 scans before that correction in the area 2 is 1.28. After the correction, the average ratio in area 2 is improved to 1.01 that is very close to the average ratio 1.04 in the area 1, but slightly overcorrected if Z_{upper}/Z_{lower} ratio in area 1 is considered as the ground truth. These results demonstrate that the proposed method is quite stable and can reasonably compensate the power lost in the blocked area.

5. Discussion

a. Data quality

Data quality is extremely important for the performance of this method. Several data quality control steps are embedded in the algorithm. First, ground clutter is filtered out in the dataset by NCAR data quality control processor. Second, observed Φ_{DP} is smoothed along the radial and the gaps (in Φ_{DP}) due to weak signal are filled by linear interpolation (Ryzhkov and Zrnic 1996). Then only the reflectivity factor with high cross-correlation coefficient and high signal-to-noise ratio is selected for the estimation of the parameters *a* and a_B. The entire quality control process helps avoid contamination by ground clutter and non-meteorological scatterers and to reduce the uncertainty of radar measurements in the weak signal regions.

b. Differences in BBFs

It is noticeable that there are some disagreements on BBFs derived from DEM data and our method in Fig. 2b. We think these differences may be due to the following reasons:

1) The parameter *b* in the Eq. (1-8) is not constant for all different types of rain and can be affected by variability of rain drop size distributions;

2) The spatial resolution of DEM is not high enough to describe the terrain profile of the actual blockage;

3) The BBF in DEM data is calculated from the one-way beam pattern whereby the blocked fraction is normalized by the 3dB beam cross section. The BBF estimated by our method is the actual estimate not sensitive to the vertical profile of the blockage;

4) There are errors in the radar measurements, such as radar antenna positioning and contributions from sidelobes;

5) Trees, buildings, and other objects which are not accounted in DEM may cause extra blockage;

6) Multiple blockages along the beam (such as two or more mountain ranges) are not considered at this time;

7) Attenuation caused by rain has not been considered.

c. Future work

The results presented in this paper have demonstrated successful retrieval of BBF using the consistency between K_{DP} and Z. Still several issues that should be addressed remain.

1) Currently the algorithm has been applied to selected individual scans. However, if there are no radials free of partial beam blockage, or if precipitation is not present along the blocked radial the correction can not be made. The algorithm can be extended from the current local status to a connected global approach. For a relatively long-lasting precipitation event over radar, a mean BBF for each azimuth/elevation could be obtained over several sequential radar scans. Then these mean BBFs can be stored in a correction table for each beam position in a volume scan. These would provide a reasonable correction along beams with small total Φ_{DP} and/or weak radar echoes. Further, by gathering enough BBF data over a period of time, climatological BBF table can be made.

2) Rain gauge observations in the area affected by beam blockage could be used to verify the corrected reflectivity through QPE. The results can help improve the performance of beam blockage correction method.

3) The impact of DSD variability and temperature on the performance of the suggested method should be quantified using theoretical simulations and radar measurements for different types of rain.

4) Combining with ground clutter detection algorithm, this algorithm can dynamically estimate BBF beyond the range location where ground clutter is detected. The idea is to exploit the fact that at these locations the clutter often partially blocks the beam.

5) Extension of the method to the cases with significant attenuation in rain (and /or shorter radar wavelengths) could be conducted.

7. Conclusion

In this paper we have proposed a novel method to estimate BBF. By integrating the self-consistency relation between K_{DP} and Z along radar beam, the immunity of total differential phase $\Delta\Phi_{DP}$ to partial beam blockage is directly used to estimate the loss of reflectivity factor measurements.

Instead of using the self-consistency relation to restore reduced Z at individual radar gate, the total differential phase $\Delta\Phi_{DP}$ and integration of measured reflectivity are adopted to directly estimate BBF for each radar beam in the blocked area. The merits of this method are: (1) it reduces the variability of parameters *a* due to different rain drop size distribution (i.e. different precipitation types); (2) it avoids the uncertainty caused by fluctuations in the Φ_{DP} or K_{DP} measurements.

The results of applications of the proposed method on the SPOL observations in the SoWMEX/TiMREX and the comparison with DEM shows the capability to estimate BBF in the beam blockage area and the advantage over DEM in the presence of high rise buildings. It provides an alternative and promising way to restore lost portion of reflectivities due to partially blocked beams. This is significant as more and more radar are being deployed near or in the urban area with many high rise buildings. But comparing to DEM method, the major disadvantage is that BBF derived based on the proposed method cannot be obtained instantly for a dual-polarimetric radar, it needs a "warm up" period for the radar with high quality measurements in a strong enough rainfall environment.

The proposed method has been quantitatively evaluated as well. By comparing the Z_{upper}/Z_{lower} ratios in between the blocked area and unblocked area, we found that the average Z_{upper}/Z_{lower} ratio in the blocked area is improved from 1.28 to 1.01, which is very close to 1.04 obtained in unblocked area after using our method. This result is the average from 45 SPOL radar volume scans in three rainfall events. The steadiness of parameter *a* and the BBFs at the azimuth of 300^{o} over about 50 scans observed in 3 rainfall events has illustrated the robustness of the method.

It is worth mentioning that the proposed method is beam based and can be applied not only to volume scan, but also sector scans, adaptive scans, and RHI scans.

Eventually, the method opens up a potentially promising avenue for operational application as the WSR-88D network is being upgraded with dual-polarimetric capability. The application of the method could make improvements in the accuracy of radar QPE as well as VIL estimation in the mountainous region where radar beams are significantly blocked.

Acknowledgements. The authors extend their thanks to Carrie Langston and Ami Arthur, who help us to generate the DEM for SPOL in Taiwan. We also want to thank Pin-Fang Lin, scientist from Central Weather Bureau of Taiwan who provided the SPOL observation data in SoWMEX experiment, and Scott Ellis, scientist from NCAR who provided the SPOL radar calibration information. Funding for the CIMMS author came from NOAA/Office of Oceanic and Atmospheric Research under NOAA-University of Oklahoma Cooperative Agreement NA17RJ1227, U.S. Department of Commerce.

References

Andrieu, H., J.D. Creutin, G. Delrieu, and D. Faure, 1997: Use of a weather radar for the hydrology of a mountainous area. 1. Radar measurement interpretation. *J. Hydrol* **193**, 1–25

Bech, J., B. Codina, J. Lorente, and D. Bebbington, 2003: The sensitivity of single polarization weather radar beam blockage correction to variability in the vertical refractivity gradient. *J. Atmos. Oceanic Technol.*, **20**:845–855.

Bringi V., and V. Chandrasekar, 2001: *Polarimetric Doppler Weather Radar.* Cambridge University Press, 636 pp.

Carey, L. D., R. Cifelli, W. A. Petersen, and S. A. Rutledge, 2000: Preliminary report on TRMM-LBA rainfall estimation using the S-Pol radar.Dept. of Atmospheric Science Paper 697, Colorado State University, Fort Collins, CO, 19 pp. [Available online at http://radarmet.atmos.colostate.edu/trmm_lba/spol_rain_info/PrelimRptLBASPOLrain.pdf].

Creutin, J. D., H. Andrieu, and D. Faure, 1997: Use of a weather radar for the hydrology of a mountainous area. Part II: Radar measurement validation. *J. Hydrol.*, **193**:26–44.

Doviak, R., and D. Zrnic, 2006: *Doppler Radar and Weather Observations.* 2nd ed. Dover Publications, 592 pp.

Giangrande, S. E. and A. V. Ryzhkov, 2005: Calibration of dual-polarization radar in the presence of

partial beam blockage. *J. Atmos. Oceanic Technol.*, **22**:1156–1166.
Goddard, J. W. F., J. Tan, and M. Thurai, 1994: Technique for calibration of meteorological radars using differential phase. *Electron. Lett.*,**30**:166–167.
Kucera, P.A., W.F. Krajewski, and C.B. Young, 2004: Radar beam occultation studies using GIS and DEM technology: an example study of Guam. *J. Atmos Oceanic Technol.,* **21**, 995–1006
Lang, T., S. Nesbitt, and L. Carey, 2009: On the correction of partial beam blockage in polarimetric radar data. *J. Atmos. Oceanic Technol*., **26**, 943 – 957.
Lang, T. J., Stephen W. Nesbitt, Lawrence D. Carey, 2009: On the Correction of Partial Beam Blockage in Polarimetric Radar Data. *J. Atmos. Oceanic Technol.*, **26**, 943–957.